

Alexander K. Hartmann, Dieter W. Heermann
 Institut für Theoretische Physik
 Ruprecht-Karls-Universität Heidelberg
 Philosophenweg 19
 69120 Heidelberg, Germany
 (December 1, 1998)

We present a new heuristic model which describes the diffusion of noble gas atoms inside a polymer matrix. The motion of the gas atoms consists of movements inside small areas called *traps* and of *hops* between different traps. Whether an atom enters another trap during a MD simulation is determined by observing a new quantity called *cage overlap*. This criterion is independent of size, time and temperature scales of the system. The resulting motions are quantitatively described by probability distributions and correlation functions. We measure these distributions for three example systems of helium, argon and krypton atoms inside a polyethylene matrix using MD simulations. Then we verify the model by comparing results from direct simulations of the *hopping model* with initial results from the MD.

61.25.H, 66.10.C, 07.05.T

I. INTRODUCTION

In the past years much progress was made in the computer simulation of the motion of small gas molecules (or *penetrants*) in polymer materials, a review can be found in¹. Molecular Dynamics (MD) simulations of polymer systems were investigated to study qualitative aspects of the diffusion process²⁻⁷. Using detailed modeling of all atoms in the system it is even possible to reproduce quantitatively experimental results within experimental accuracy⁸⁻¹².

From the early MD simulations we know that the gas transport through dense polymer matrices proceeds by a hopping mechanism^{2,4,5,9} between different voids (or *cavities* or *traps*). A penetrant was said to hop if it traveled within a certain amount of time longer than a temperature and material dependent distance. This hopping mechanism led to the development of a Transition State Approach (TSA)^{13,14}. There the motion of the penetrants is coupled to the elastic motion of dense polymers, but is independent from the structural relaxation of the polymer matrix. So the approach is not applicable to higher temperatures where the polymer systems is a melt.

The aim of this article is to introduce a new criterion for the detection of hops of the penetrants in a MD sim-

ulation which is independent of temperature and time- and length-scales. The main idea is to look not at the motion of the gas itself, but to observe its environment. If the environment changes much the penetrant moves to a new void. This leads to the definition of a new quantity called *cage overlap*.

For more information on general types of systems where particles diffuse by staying locally confined for a while and then making longer jumps to a new confining region, see for example¹⁵⁻¹⁸.

The outline of the paper is as follows: We start by giving the basic computational methods like simulation algorithm and force fields. Then we proceed by defining the cage overlap. We introduce quantities that allow the measurement the gas hopping process quantitatively. Results from MD simulations of helium, argon and krypton in polyethylene (PE) are given. These data are used to simulate the motion of the penetrants directly and the results are compared with the original MD runs.

II. COMPUTATIONAL METHODS

We performed our sample simulations using the Molecular Dynamics method with the Velocity-Verlet algorithm (time step 2.1 fs) and the Nosé-Hover¹⁹ algorithm to hold the temperature at T=450 K (T*=7.5 in reduced units). The united atom model^{20,21} (or Bead-Spring model) was used to describe the PE-system, i.e. the hydrogen-atoms of the polymers are not explicitly included. This does not cause any trouble, because our aim is to test our model and not to reproduce experimental diffusion constants with high accuracy.

The force field is given by the following expression for the potential energy

$$E_{\text{pot}} = \sum_{\text{bonds}} \frac{k_b}{2} (l - l_0)^2 + \sum_{\text{angles}} \frac{k_\Theta}{2} (\cos\Theta - \cos\Theta_0)^2 + \sum_{\text{pairs}} 4\epsilon \left[\left(\frac{\sigma}{r} \right)^{12} - \left(\frac{\sigma}{r} \right)^6 \right] \quad (1)$$

The intra molecular potential function comprises harmonic bond and harmonic angle interactions, but we have no torsional potential.

The interactions between monomers separated by more than two bonds and the interactions where the gas atoms

participate are described by Lennard-Jones (LJ) potentials. All LJ interactions were truncated at $r_{cut} = 1.5\sigma$ to speed up the calculations. The force field parameters^{21,22} are shown in table I. For the LJ interaction between different species α, β the Lorentz-Berthelot combining rules²³ were used

$$\sigma_{\alpha, \beta} = \frac{\sigma_{\alpha} + \sigma_{\beta}}{2}, \quad \epsilon_{\alpha, \beta} = \sqrt{\epsilon_{\alpha}\epsilon_{\beta}} \quad (2)$$

The mixture consisted of 680 PE chains each 39 monomers long and 80 gas atoms inside a cubic box of linear size $9.4nm$ ($L^* = 23.8$ in reduced units). The rather large system should keep the finite size effects small. This resulted in a density of $0.74 g/cm^3$ ($\rho^* = 1.97$ in reduced units) without the atoms. The system was set up by folding 86 random walks of length 39 with fixed angle Θ_0 between two steps into a simulation box of $4.7nm$. Using a Lennard-Jones Potential which was set to a constant value for $r < r_{min}$ the system was equilibrated, while r_{min} was stepwise reduced to zero. Afterwards 2 chains were removed and replaced by 5 gas atoms each. The system then equilibrated for 1ps so that every gas atom moved on average once through the hole system. Then the system was doubled in each direction and the equilibration process repeated.

We use $\underline{R}_i(t)$, $\underline{r}_m(t)$ to denote the positions of atom i and monomer m at time t . The diffusion constant D was measured using the mean square displacement $\langle |\underline{R}_i(t) - \underline{R}_i(0)|^2 \rangle$ where $\langle \dots \rangle$ denotes an average over all gas atoms and all time origins every 10 MD steps. For long enough times the behavior of the penetrant motion becomes diffusive and the Einstein relation²⁰ holds

$$\langle |\underline{R}_i(t) - \underline{R}_i(0)|^2 \rangle = 6Dt \quad (3)$$

We used plots of $\langle |\underline{R}_i(t) - \underline{R}_i(0)|^2 \rangle / t$ to examine the diffusion of the penetrants.

III. DEFINITION OF THE CAGE OVERLAP

Figure 1 shows the path of a sample helium atom inside the polyethylene matrix. The quantities in all figures are measured in reduced units. Figure 2 displays snapshots of the movement of the atom (large) and some of its surrounding polyethylene monomers (small). The atom's positions at the snapshot moments are marked by circles in figure 1

Within the first 600 MD steps the atom oscillates within an area restricted by the surrounding monomers which are shown in dark blue. Then it travels (steps 600 to 1200) to another area (light blue) where it starts to oscillate again. At step 1650 it starts traveling to a third area.

So the hopping mechanism between different traps is clearly visible even at high temperatures and flexible chains. This behavior also can be seen from the kinetic

energy of the atom as function of time (Figure 3, in reduced units). While it is inside a trap it travels only during short time intervals without stopping (from configuration 0 to 600 and from configuration 1100 to 1650). An atom i is said to *stop* if its kinetic energy $E_i^{kin}(t)$ at time t is below a certain threshold value E^{th} . We used $E^{th} = 0.25T^*$. Formally the time s_i^n of the n 'th stop of atom i is defined as (our simulations start at $t = 0$):

$$\begin{aligned} s_i^1 &= \min \{ t > 0 | E_i^{kin}(t) < E^{th} \} \\ s_i^{n+1} &= \min \{ t > s_i^n | E_i^{kin}(t) < E^{th}, \\ &\quad \exists t^*, s_i^n < t^* < t : E_i^{kin}(t^*) > E^{th} \} \end{aligned} \quad (4)$$

The first stop is given by the first time the energy is below the threshold. The other stopping times are defined by recursion: stop $n + 1$ is the first time (i.e. the *minimum* time) after the n th stop, where the energy is below the threshold *again*. Thus in between there must be a time ($\exists t^*$) where the kinetic energy is higher than the threshold (at time t^*). This prevents the stops being successive time steps, if the energy is below the threshold for some time interval.

The stops of the atom are indicated by vertical dashed lines in Figure 3. While the atom travels between traps, no stop occurs (from step 600 to 1100 and after step 1650).

In Figure 4 the distance $d_i(t)$ of the atom's position to the position where it stopped the last time is shown ($s_i^n < t \leq s_i^{n+1}$)

$$d_i(t) = |\underline{R}_i(t) - \underline{R}_i(s_i^n)| \quad (5)$$

While the atom is inside a trap it doesn't travel far. The diameter of the free volume which is available is about 0.5 units = 0.197 nm. During hops the atoms moves much further. From these distances the average size of a trap and the average distance between two traps can be measured.

In order to describe the movement of an atom by a stochastic model consisting of jumps between traps, we need a formal definition of a trap, i.e. a criterion which decides whether an atom has entered a new trap. This criterion is needed, because we want to analyze simulations automatically without *looking* at the movement of the atoms.

The simplest definition of a trap uses the *cage* $C_i(t)$ for an atom i at time t , which is just the set of monomers, given by their indices m , which are located within a given distance r_{cage} from the atom:

$$C_i(t) := \{ m | |\underline{R}_i(t) - \underline{r}_m(t)| < r_{cage} \} \quad (6)$$

We used $r_{cage} = 1.8\sigma_{CH_3, X}$ for gas X (He, Ar, Kr) so that r_{cage} is about the sum of r_{cut} and the average size of a trap.

The criterion which indicates if an atom has entered a new trap should be independent of time and length scales of the system. So it wouldn't be useful to use the

time between two stops or the distance the atom traveled between two stops as indicator that an atom has entered a new trap.

Instead we look at the cage. To determine how much the cage of an atom has changed, we calculate the *overlap* $q_i(t)$ of the actual cage with the cage $C_i(s_i^n)$ which was around the atom when it stopped last time, i.e. the fraction of the monomers in the actual cage, which were also in $C_i(s_i^n)$ (for $s_i^n < t \leq s_i^{n+1}$):

$$q_i(t) := |C_i(s_i^n) \cap C_i(t)| / |C_i(s_i^n)| \quad (7)$$

where $|\dots|$ denotes here the number of elements in a set. (We assume $q_i(t) := 1$ ($t \leq s_i^1$) to obtain formal consistency). The time dependence of the cage-overlap $q_i(t)$ for the example atom is shown in Figure 5. While the atom is located inside a trap, the cage doesn't change very much between two stops. But when the atoms travels to a new trap, the set of surrounding monomers changes drastically.

So we assume that an atom has entered a new trap if the overlap is smaller than a specific 'critical' value q_{crit} . We used $q_{crit} = 0.5$. (Our final results for the simulation using the *hopping model*, doesn't depend very much on the value of q_{crit} in the interval $[0.3, 0.7]$) So the time c_i^n the atom i enters the n 'th trap can be defined as

$$\begin{aligned} c_i^1 &:= \min\{t > 0 | q_i(t) < q_{crit}, \exists m : t = s_i^m\} \\ c_i^{n+1} &:= \min\{t > c_i^n | q_i(t) < q_{crit}, \exists m : t = s_i^m\} \end{aligned} \quad (8)$$

The expression $\exists m : t = s_i^m$ means: only times where an atom stops are evaluated to determine the times an atom enters a trap. The definition is recursive again: The first time the overlap falls below q_{crit} gives c_i^1 . Time c_i^{n+1} is the first time higher than c_i^n with $q_i(t) < q_{crit}$. By definition the overlap jumps to 1 immediately after a stop, so this feature has not to be checked, as it was done for the kinetic energy in the definition of s_i^n (5).

For the further calculations only the times an atom enters a new trap are needed, but no formal definition of a trap itself.

Figures 6 and 7 indicate the consistency of this criterion. Figure 6 displays the overlap $q_i^*(t)$ of the actual cage with the cage the atom was in, when it entered the actual trap (for $c_i^n < t \leq c_i^{n+1}$):

$$q_i^*(t) := |C_i(c_i^n) \cap C_i(t)| / |C_i(c_i^n)| \quad (9)$$

This overlap remains close the value of the former defined overlap $q_i(t)$. Figure 7 shows the distance $d_i^*(t)$ of atom i 's position at time t to the position where it was at the time it entered last time a new trap (for $c_i^n < t \leq c_i^{n+1}$):

$$d_i^*(t) = |\underline{R}_i(t) - \underline{R}_i(c_i^n)| \quad (10)$$

Comparing to Figure 4 we can see that, while the atom is inside a trap, it doesn't travel much farther than between two stops. This is another sign that the atom is really trapped.

The main idea of a model describing the diffusion of atoms through the polymer host is to describe the motion by probability distributions which depend on parameters like polymer host material, density and temperature. The first aim is to identify the suitable quantities describing the hopping between traps by calculating their probability distributions and testing if a direct simulation of the gas atoms using this distributions results in the same diffusion as in the full simulation.

We have tested two models which are displayed symbolically in Figures 8 and 9. Both models describe the motion of an atom as a sequence of mesoscopic hops.

The first model (Figure 8) consist of one type of hop: From the position where an atom enters a trap to the position where it enters the next trap. The distance $r_{h1}(i, n)$ of the n 'th hop of atom i and the time $\Delta t_{h1}(i, n)$ that hop lasts are given by:

$$\begin{aligned} \Delta t_{h1}(i, n) &:= c_i^{n+1} - c_i^n \\ r_{h1}(i, n) &:= |\underline{R}_i(c_i^{n+1}) - \underline{R}_i(c_i^n)| \end{aligned} \quad (11)$$

So the model is quantitatively given by the probability distributions of r_{h1} and Δt_{h1} . We don't show these distributions because we use this model only to compare its final results with the detailed model which follows now.

The model shown in Figure 9 consists of two type of movements: One movement from the position where an atom enters a trap to the position where the trap is left (*intra movement/hop*) and another hop from there to the next trap (*inter hop*). The moment l_i^n when an atom i leaves its n 'th trap is defined as the last stop of the atom before it stops the first time inside a new trap. Formally this time is given by: $l_i^n := s_i^m$ if $s_i^{m+1} = c_i^{n+1}$.

The durations $\Delta t_c(i, n)$, $\Delta t_h(i, n)$ of these two hop types for atom i and the n 'th trap are given by:

$$\begin{aligned} \Delta t_c(i, n) &:= l_i^n - c_i^n \\ \Delta t_h(i, n) &:= c_i^{n+1} - l_i^n \end{aligned} \quad (12)$$

The distances $r_c(i, n)$ and $r_h(i, n)$ are

$$\begin{aligned} r_c(i, n) &:= |\underline{R}_i(l_i^n) - \underline{R}_i(c_i^n)| \\ r_h(i, n) &:= |\underline{R}_i(c_i^{n+1}) - \underline{R}_i(l_i^n)| \end{aligned} \quad (13)$$

We also measured the correlation between the hopping durations and distances, i.e. the functions $r_c(\Delta t_c)$ and $r_h(\Delta t_h)$ and the distributions of the distances. During our simulations we observed that the use of these correlations functions instead of the distance distributions gave the same results but was faster, so we used the correlation functions.

Because not every time an atom hops to a new trap, it moves inside that trap, we measured the probability p_{cont} that the atom hops to a new trap just after it has reached a trap (then the time an atom leaves a trap is equal to the time the atom has entered the trap: $l_i^n := c_i^n$):

$$p_{cont} := P(q_i(s_i^{n+1}) < q_{crit} | \exists m : c_i^m = s_i^n) \quad (14)$$

So p_{cont} is the probability that the overlap of atom i at stop $n + 1$ is below the threshold value q_{crit} , if at the stop before (n) the atom has entered a new cage ($\exists m : c_i^m = s_i^n$).

A more detailed description is achieved if one measures the angles between two successive moves.

If the atom i moves inside the n th trap, the angle $\beta_{hc}(i, n)$ between a hop to the trap (from time $t = l_i^{n-1}$ to $t = c_i^n$) and the motion inside the trap (from $t = c_i^n$ to $t = l_i^n$) is

$$\cos \beta_{hc}(i, n) := \frac{(\underline{R}_i(l_i^n) - \underline{R}_i(c_i^n)) \cdot (\underline{R}_i(c_i^n) - \underline{R}_i(l_i^{n-1}))}{|\underline{R}_i(c_i^n) - \underline{R}_i(l_i^{n-1})| |\underline{R}_i(c_i^n) - \underline{R}_i(l_i^n)|} \quad (15)$$

The angle $\beta_{ch}(i, n)$ between the motion in the trap and the hop to the next trap is given by

$$\cos \beta_{ch}(i, n) := \frac{(\underline{R}_i(c_i^{n+1}) - \underline{R}_i(l_i^n)) \cdot (\underline{R}_i(l_i^n) - \underline{R}_i(c_i^n))}{|\underline{R}_i(c_i^{n+1}) - \underline{R}_i(l_i^n)| |\underline{R}_i(l_i^n) - \underline{R}_i(c_i^n)|} \quad (16)$$

If atom i doesn't move inside trap n we define the angle $\beta_{hh}(i, n)$ between two successive hops to a cage

$$\cos \beta_{hh}(i, n) := \frac{(\underline{R}_i(c_i^{n+1}) - \underline{R}_i(c_i^n)) \cdot (\underline{R}_i(c_i^n) - \underline{R}_i(l_i^{n-1}))}{|\underline{R}_i(c_i^{n+1}) - \underline{R}_i(c_i^n)| |\underline{R}_i(c_i^n) - \underline{R}_i(l_i^{n-1})|} \quad (17)$$

So the full model is represented by the probability density functions (pdf) for Δt_c and Δt_h , by the functions $r_c(\Delta t_c)$ and $r_h(\Delta t_h)$, by the probability p_{cont} and by the probability distributions for the angles β_{ch} , β_{hc} and β_{hh} .

The direct simulation of the atoms using this model is done as follows: At $t = 0$ all atoms are assumed to be in a trap. For each atom a duration is drawn from the probability distribution of Δt_c ; this is the time of the next event (*event time*) for that atom. A *distance* is calculated using $r_c(\Delta t_c)$. The atoms are sorted into an *event list* in ascending order of their *event times*.

In a loop the main simulation step is performed: The atom with the smallest event time is taken from the list. The atom is moved in a certain direction about the *distance*. This direction can be drawn randomly or according to the distribution for the angles described above. If the atom is *in* a trap, it will travel *between* two traps at the next event. If it is *between* two traps, it will be with probability p_{cont} *between* two traps and otherwise *in* a trap at the next event. A new duration is calculated from the probability distributions of Δt_c or Δt_h and added to the event time, and a *distance* is calculated using $r_c(\Delta t_c)$ or $r_h(\Delta t_h)$. Finally the atom is reinserted into the *event list*.

V. RESULTS

We tested our models by simulating polyethylene systems together with helium, argon or krypton guest atoms during 100000 MD steps. In this section we show the probability distributions for the hop durations and the correlation functions. With these results we simulated the diffusion of the atoms using the second hopping model. Finally we compare the diffusion constants resulting from the MD simulation and the hopping model.

The probability density functions (pdf) of the time an atom stays inside a trap are shown in Figure 10 for helium and argon (krypton stays even longer than argon in a trap). The average time an argon atom stays inside a trap is about four times higher than the duration for helium. All functions are described well by a convolution of two exponential pdfs, which is given by:

$$f_{\lambda_1, \lambda_2}(t) = \frac{\lambda_1 \lambda_2}{\lambda_2 - \lambda_1} (e^{-\lambda_1 t} - e^{-\lambda_2 t}) \quad (18)$$

The resulting parameters for the three atom types are shown in table II.

During the simulation using the second hopping model the durations according f_{λ_1, λ_2} can be drawn directly: given two $[0, 1]$ uniform distributed numbers u_1, u_2 , the time an atom stays inside a cage is calculated using²⁴:

$$\Delta t_c = -\frac{1}{\lambda_1} \ln(u_1) - \frac{1}{\lambda_2} \ln(u_2) \quad (19)$$

In Figure 11 the pdfs of the inter cage hopping durations Δt_h of helium and argon are displayed. The average duration times of argon atoms are about two times the values of helium. This proportion is smaller than in the case of Δt_c (see Figure 10) and indicates that the process of escaping a trap is more influenced by the size of an atom than the process of moving to another trap.

Because of the poor statistics we were not able to calculate a consistent fit function for these pdfs. So we used the empirical distribution directly for the simulation of the hopping model. We used the rejection method²⁴ for drawing times according these distributions.

The dependency of the inter- and intra-hopping distances of the hopping durations are shown in Figure 12 and 13 for helium and argon. We approximated these functions by $r(\Delta t) = c * \ln(f * \Delta t + s)$. They are shown in table II. Comparing the two figures one notices that helium always moves faster than argon and that inside a trap the motion of all noble gases is much slower than outside.

The distributions for the angles between two successive hops for helium can be seen in figure 14. The probability for a reflection is higher than the probability for continuing the movement in the same direction. The distribution for β_{hh} is steeper. But since the fraction of two consecutive hops to a cage is not very high and because the differences between the distributions are of the order of the numerical uncertainty of our other parameters, we

used a superposition of all three distributions for all types of movements.

We simulated the hopping model using these parameters. The result for helium is shown in Figure 15, where the mean square displacement per time step as function of time is shown. For $t \rightarrow \infty$ this quantity should converge to six times the diffusion constant D . For comparison we included results from the one hop model and a simple model, which uses only time and distance distributions for the movements between two stops. For all three models we performed simulations with and without using the angle distributions. For all models the second case results in a more or less straight line, indicating that the particles are in the diffusive regime. The resulting diffusion constants are ranging from $D = 3.56 \cdot 10^{-4} \text{cm}^2/\text{s}$ to $D = 6.01 \cdot 10^{-4} \text{cm}^2/\text{s}$. For the angular models one can see a second regime for longer times. There the motion is slower than in the first regime, because of the influence of the angle distributions. The transition from short to long time movement is determined by the time distributions $\Delta t_{xx}(i, n)$. For the simple model this is the time $\Delta t_s := s_i^{n+1} - s_i^n$ between two stops, for the one hop model the time between two trap hops Δt_{h1} and for the two hop model a combination of the times Δt_c and Δt_h .

For short times all three models are not describing the motion of the atoms, because in the MD simulation the atoms can move free on short time scales inside a trap, so the motion is faster than a diffusion. For long time scales, when the atoms are in the diffusive regime, all three models describe the motion well. The transition between the two regimes starts where the lines for the angular and non angular variants split up. The transition is described the best by the two hop model. In the one hop model the transition is slightly later. But for the simple model the transition is definitely to early, because the diffusion constant begins to fall when in the MD simulation it is still rising. This is another indication that atoms are really caught in traps and move by jumps between these traps.

In Figures 16 and 17 the result of the angular models for argon and krypton are shown together with the result of the MD simulation. Here the resulting diffusion constants for the simple and the two hop model reproduces the MD simulation very well too, the one hop model is a little worse. Here the simple model suffers from the early transition between the two regimes as well. The resulting diffusion constants are ranging from $D = 1.07 \cdot 10^{-4} \text{cm}^2/\text{s}$ to $D = 1.25 \cdot 10^{-4} \text{cm}^2/\text{s}$ for argon and from $D = 8.79 \cdot 10^{-5} \text{cm}^2/\text{s}$ to $D = 9.96 \cdot 10^{-5} \text{cm}^2/\text{s}$ for krypton. All our diffusion constants are about one order of magnitude or even higher above results from experiments and precise simulations¹, because we use a simple model and a high temperature.

VI. SUMMARY

In this paper we presented a new empirical model describing the diffusion of noble gas atoms through a mobile polymer host by jumps in and between traps. The cage overlap was introduced resulting in a temperature and time-/length-scale independent criterion whether a penetrant performs a jump in each moment. Another advantage over previous definitions is that not the whole system does not have to be scanned in the search for the voids, since the information about which monomer is in the vicinity of each gas atom is already collected during the MD simulation for building the nearest-neighbor tables.

We measured the distributions and parameters for helium/argon/krypton inside a dense system of short polyethylene chains. We simulated the new model directly. The gas diffusion constant of the MD simulation was reproduced very well. We compared some variants of the hopping model. The variant which distinguishes between the atoms being inside and outside a trap and includes the angle distributions between two successive hops reproduced the MD results the best. Because the hopping models reproduce the transition between short time and long time behavior much better than the simple model, the hopping model is likely to be a good description of the motion of atoms inside polymer matrices. Using the cage overlap criterion a more detailed analysis of MD simulations can be achieved.

We will perform MD simulation of larger systems with longer runs in the future. For this purpose we will use a parallel program which was partly developed during a visit at the Edinburgh Parallel Computing Center. This enables us to describe the motion of gas atoms inside polymer systems with high accuracy. We will use different parameters of temperature, chain lengths, densities and materials for the simulations. So it should be possible to learn how different conditions and material properties are reflected in the diffusion process.

VII. ACKNOWLEDGEMENTS

We would like to thank Kurt Binder, Kurt Kremer and Florian Müller-Plathe from Mainz for valuable discussions. This work was supported by the Bundesministerium für Bildung und Forschung (BMBF) in the framework of the project “Computer Simulation Komplexer Materialien” under grant no. 03N8008D, the European Union project “Computational Modeling of Diffusion in Amorphous Media” (CIPA-CT93-0105) and by the Graduiertenkolleg “Modellierung und Wissenschaftliches Rechnen in Mathematik und Naturwissenschaften” at the *Interdisziplinäres Zentrum für Wissenschaftliches Rechnen* in Heidelberg.

- ¹ A.A. Gusev, F. Müller-Plathe, W.F. van Gunsteren and U.W. Suter, *Adv. Polym. Sci.* **116**, 207 (1994)
- ² H. Takeuchi and K. Okazaki, *J. Chem. Phys.* **92**, 5643 (1990)
- ³ H. Takeuchi, *J. Chem. Phys.* **93**, 4490 (1990)
- ⁴ J. Sonnenburg, J. Gao and J.H. Weiner, *Macromolecules* **23**, 4653 (1990)
- ⁵ F. Müller-Plathe, *J. Chem. Phys.* **94**, 3192 (1991)
- ⁶ R.H. Boyd and P.V.K. Pant, *Macromolecules* **24**, 6325 (1991)
- ⁷ F. Müller-Plathe, L. Laaksonen, W.F. van Gunsteren, *J. Mol. Graph.* **11**, 118 (1993)
- ⁸ F. Müller-Plathe, *J. Chem. Phys.* **96**, 3200 (1992)
- ⁹ R.M. Sok and H.J.C Berendsen, *J. Chem. Phys.* **96**, 4699 (1992)
- ¹⁰ P.V.K. Pant, R.H. Boyd, *Macromolecules* **25**, 494 (1992)
- ¹¹ P.V.K. Pant and R.H. Boyd, *Macromolecules* **26**, 679 (1993)
- ¹² F. Müller-Plathe, S.C. Rogers, W.F. van Gunsteren, *J. Chem. Phys.* **98**, 9895 (1993)
- ¹³ A.A. Gusev, U.W. Suter, *ACS Polym. Preprints* **33**, 631 (1992)
- ¹⁴ A.A. Gusev, S.A. Arrizi, D.J. Moll, U.W. Suter, *J. Chem. Phys.* **99**, 2221 (1993)
- ¹⁵ M.F. Shlesinger, G.M. Zaslavsky and U. Frisch, *Levy Flights and Related Topics in Physics*, Springer, 1995
- ¹⁶ J. Klafter, M.F. Shlesinger, G. Zumofen, *Physics Today* **49**, 33 (1996)
- ¹⁷ D.S. Sholl and R.T. Skodje, *Physica D* **71**, 168 (1984)
- ¹⁸ J.S. Raut and K.A. Fichthorn, *J. Chem. Phys.* **103**, 8694 (1995)
- ¹⁹ S. Nosé, *J. Chem. Phys.* **81** (1984), 511–518
- ²⁰ M.P. Allen and D.J. Tildesley, *Computer Simulation of Liquids*, Clarendon Press, Oxford, 1987;
- ²¹ D. Rigby and R.J. Roe, *J. Chem. Phys.* **87** (1987), 7285–7292
- ²² B.M. Forrest and U.W. Suter, *J. Chem. Phys.* **101** 2616 (1994)
- ²³ G. C. Maitland, M. Rigby, E. B. Smith and W. A. Wakeham, *Intermolecular Forces*, Clarendon, Oxford 1981
- ²⁴ B.J.T. Morgan, *Elements of Simulation*, Chapman and Hall, London, New York 1984
6. Overlap of the actual cage of the example atom with the cage around the atom when the it entered last time a new trap.
7. Distance of the example atom to the position where it was when it entered last time a new trap.
8. Simple model for the atom movement: The atom hops between traps, the movement inside the trap is neglected.
9. More complex model for atom movement: The diffusion inside a trap and between traps are distinguished.
10. Probability density functions of Δt_c for helium and argon together with fits.
11. Probability density functions of Δt_h for helium and argon and krypton.
12. The distance of an intra-hop $r_c(\Delta t)$ as function of the time Δt_c an atom stays inside a trap.
13. The distance of an inter-hop $r_h(\Delta t_h)$ as function of the duration Δt_h of a hop.
14. The probability density functions for the angles β_{ch} , β_{hc} and β_{hh} for helium.
15. Mean square displacement of helium per time step for the MD simulation, the simple model, the one-hop and the two-hop model (with and without angle distributions). The resulting diffusions constants are ranging from $D = 3.56 \cdot 10^{-4} cm^2/s$ for the simple angular model to $D = 6.01 \cdot 10^{-4} cm^2/s$ for the one hop model.
16. Mean square displacement of argon per time step for the MD simulation, the simple model, the one-hop and the two-hop model. The resulting diffusion constants are ranging from $D = 1.07 \cdot 10^{-4} cm^2/s$ for the simple model to $D = 1.25 \cdot 10^{-4} cm^2/s$ for the one hop model.
17. Mean square displacement of krypton per time step for the MD simulation, the simple model, the one-hop and the two-hop model The resulting diffusion constants are ranging from $D = 8.79 \cdot 10^{-5} cm^2/s$ for the simple model to $D = 9.96 \cdot 10^{-5} cm^2/s$ for the one hop model.

Figure Captions

1. Path of a sample helium atom inside a PE system. The positions of the atom at times $t = 0, 400, 800, 1200, 1600, 2000$ are marked.
2. Snapshots showing the motion of an example helium atom inside a PE system during 2000 MD steps.
3. Kinetic energy (in reduced units) of the example helium atom
4. Distance (in reduced units) of the example atom's position to the position of its last stop as function of time.
5. Cage overlap for the example atom as function of time.

Bonds	l_0	k_b
$CH_2 - CH_2$	0.157 nm	$5 \cdot 10^5$ J/mol
Angles	Θ_0	k_Θ
$CH_2 - CH_2 - CH_2$	112°	$3.22 \cdot 10^7$ J/(nm ² mol)
Lennard Jones	ϵ	σ
CH_2	500 J/mol	0.394 nm
He	104 J/mol	0.258 nm
Ar	1260 J/mol	0.342 nm
Kr	2090 J/mol	0.352 nm

TABLE I. Force field parameters for Bead-Spring model.

Parameter	helium	argon	Krypton
λ_1	$23.2 \cdot 10^{-4}$	$9.25 \cdot 10^{-4}$	$2.77 \cdot 10^{-4}$
λ_2	$307 \cdot 10^{-4}$	$127 \cdot 10^{-4}$	$62.3 \cdot 10^{-4}$
p_{cont}	0.403	0.316	0.140
$r_c(\Delta t_c) : c$	0.47	0.43	0.66
f	$7.7 \cdot 10^{-3}$	$4.2 \cdot 10^{-3}$	$1.8 \cdot 10^{-3}$
s	1.79	1.15	1.06
$r_h(\Delta t_h) : c$	2.44	0.66	0.52
f	$1.3 \cdot 10^{-3}$	$5.6 \cdot 10^{-3}$	$18 \cdot 10^{-3}$
s	1.42	1.51	1.00

TABLE II. Model parameters for helium, argon and krypton

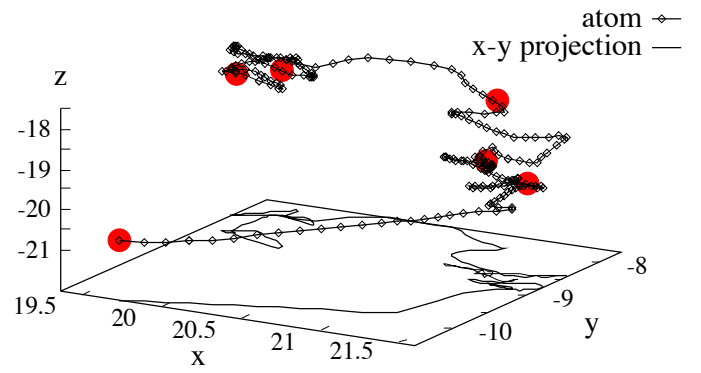


FIG. 1. Alexander K. Hartmann, J. Chem. Phys.

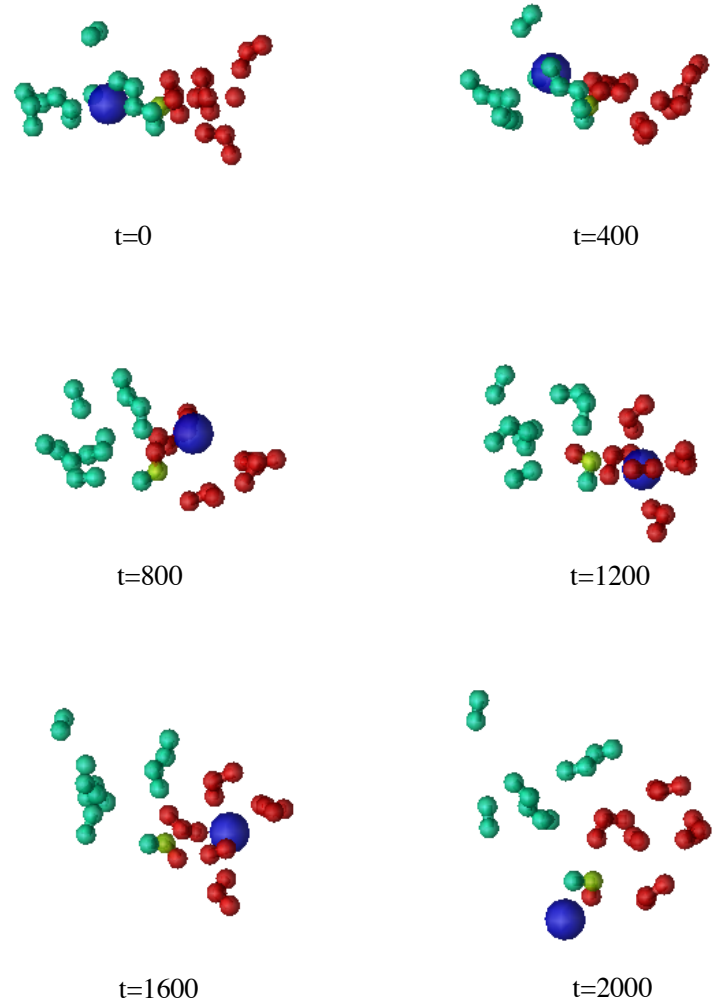


FIG. 2. Alexander K. Hartmann, J. Chem. Phys.

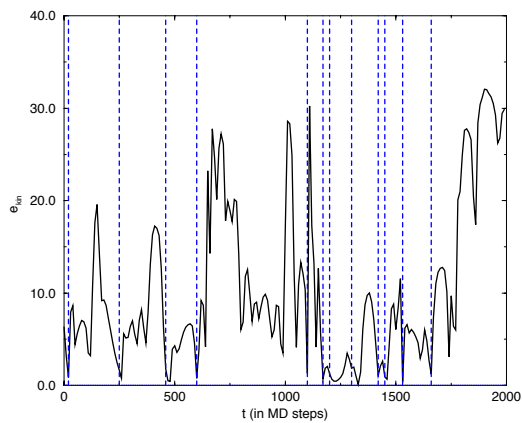


FIG. 3. Alexander K. Hartmann, J. Chem. Phys.

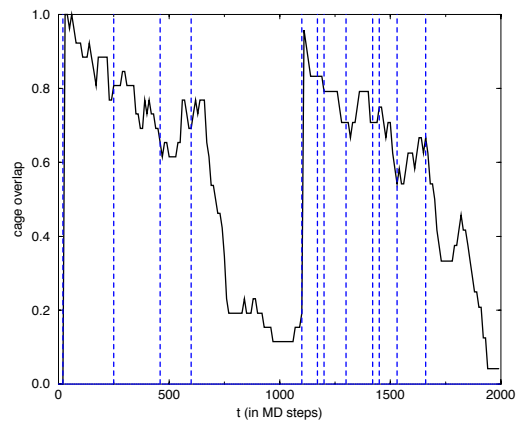


FIG. 6. Alexander K. Hartmann, J. Chem. Phys.

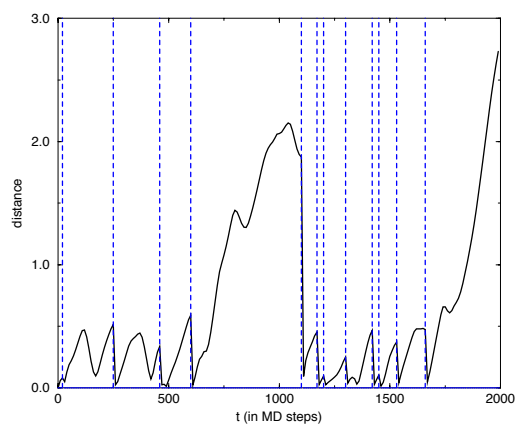


FIG. 4. Alexander K. Hartmann, J. Chem. Phys.

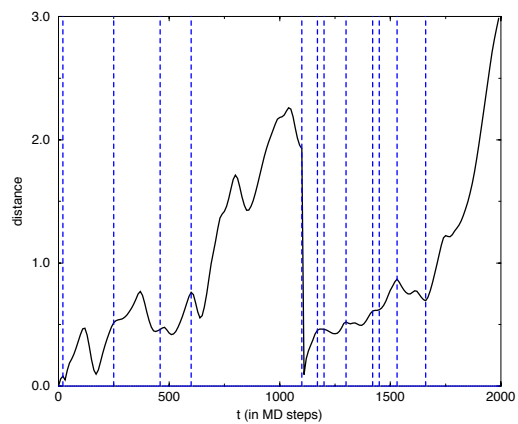


FIG. 7. Alexander K. Hartmann, J. Chem. Phys.

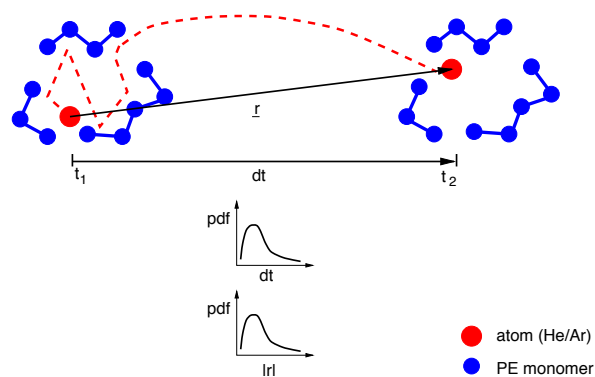
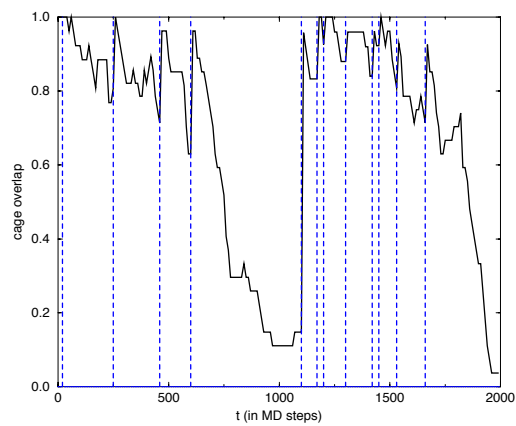


FIG. 8. Alexander K. Hartmann, J. Chem. Phys.

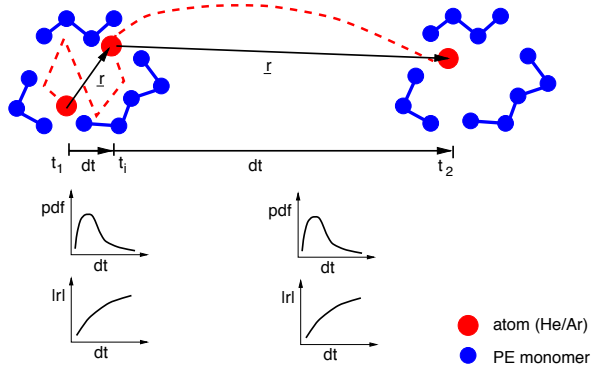


FIG. 9. Alexander K. Hartmann, J. Chem. Phys.

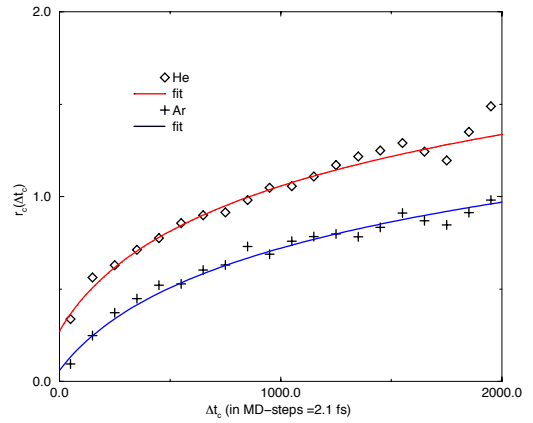


FIG. 12. Alexander K. Hartmann, J. Chem. Phys.

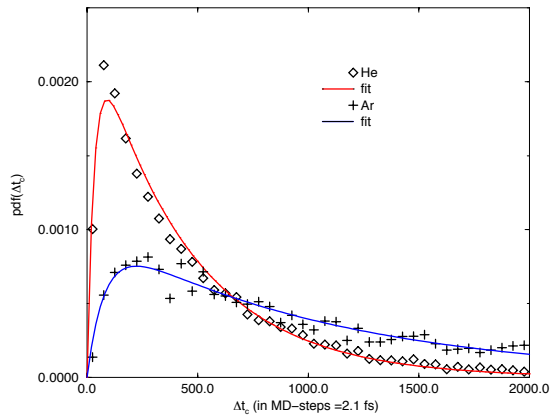


FIG. 10. Alexander K. Hartmann, J. Chem. Phys.

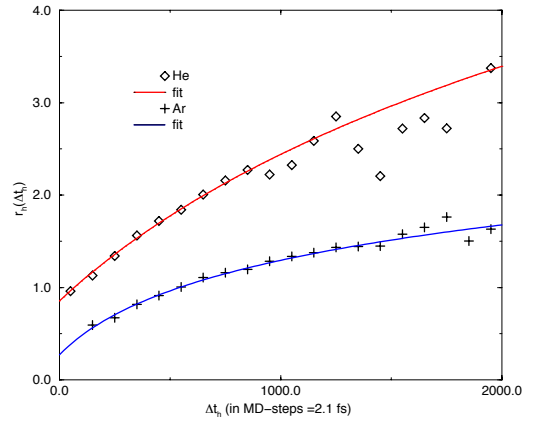


FIG. 13. Alexander K. Hartmann, J. Chem. Phys.

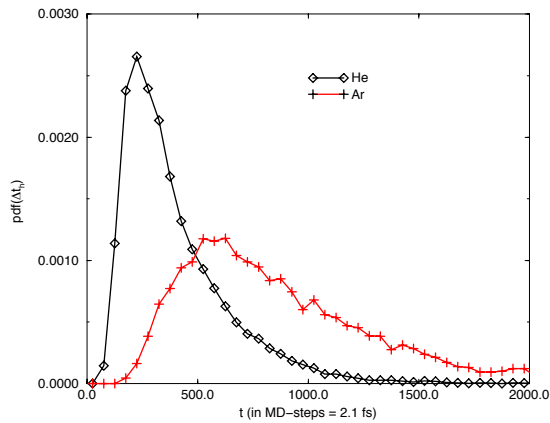
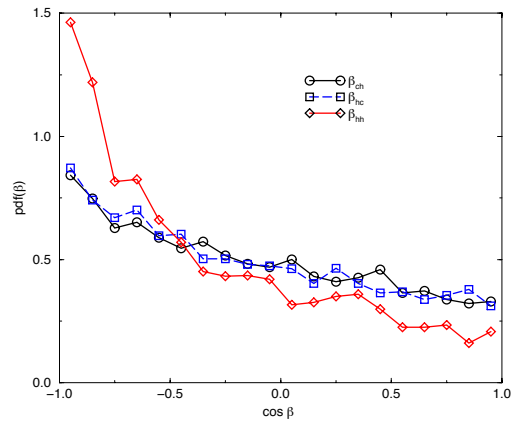


FIG. 11. Alexander K. Hartmann, J. Chem. Phys.



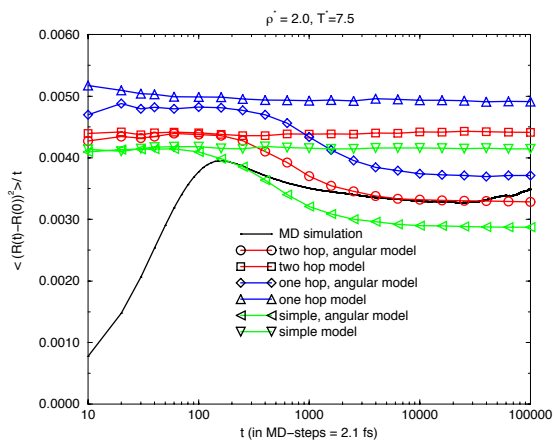


FIG. 15. Alexander K. Hartmann, J. Chem. Phys.

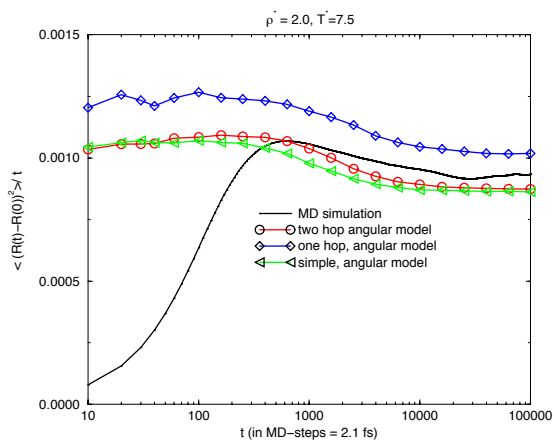


FIG. 16. Alexander K. Hartmann, J. Chem. Phys.

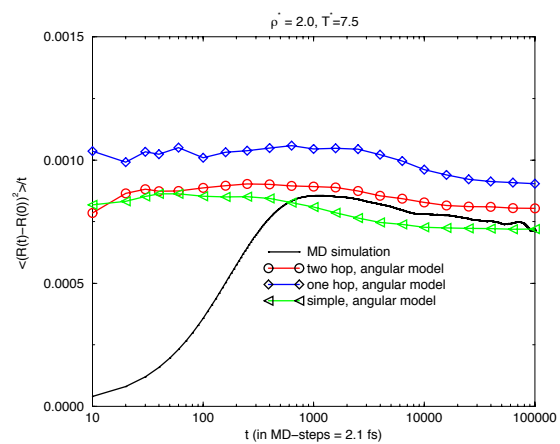


FIG. 17. Alexander K. Hartmann, J. Chem. Phys.